# Deconvolution with curvelet-domain sparsity

*Vishal Kumar*, EOS-UBC and Felix J. Herrmann, EOS-UBC*

## SUMMARY

We use the recently introduced multiscale and multidirectional curvelet transform to exploit the continuity along reflectors for cases in which the assumption of spiky reflectivity may not hold. We show that such type of seismic reflectivity is sparse in the curvelet-domain. This curvelet-domain compression of reflectivity opens new perspectives towards solving classical problems in seismic processing including the deconvolution problem. In this paper, we present a formulation that seeks curvelet-domain sparsity for non-spiky reflectivity and we compare our results with those of spiky deconvolution.

## INTRODUCTION

The forward problem of seismic imaging can be written as:

$$\mathbf{y} = \mathbf{AKm} + \mathbf{n}, \tag{1}$$

where $\mathbf{y}$ is the known data vector, $\mathbf{K}$ is the linearized Born scattering operator, $\mathbf{A}$ is the convolution operator representing source and receiver frequency characteristics, $\mathbf{m}$ is the unknown model vector (reflectivity) and $\mathbf{n}$ is zero-centered white Gaussian noise. For now, we assume that the source and receiver are omnidirectional. During the traditional processing, we first deconvolve, followed by migration in which case the estimated reflectivity is given by $\tilde{\mathbf{m}} = \mathbf{K}^\dagger \mathbf{A}^\dagger \mathbf{y}$, where $^\dagger$ denotes the pseudo inverse (some sort of approximate inverse). On the other hand, simultaneous migration and deconvolution produces the solution $\tilde{\mathbf{m}} = (\mathbf{AK})^\dagger \mathbf{y}$. Although, it is claimed that both approaches would generate the same result, they are not the same in theory (De Roeck, 2002).

Indeed in the situation where both $\mathbf{K}$ and $\mathbf{A}$ are invertible, we have $(\mathbf{AK})^{-1} = \mathbf{K}^{-1}\mathbf{A}^{-1}$ justifying the approach of deconvolution first followed by migration. However, we all know that deconvolution is an ill-posed problem whereas least-squares migration entails the inversion of an over-determined system. This means that the above identity may no longer hold as right fully pointed out by De Roeck. This paper is a first attempt to address this issue. To keep our argument simple, we assume for now that the Born scattering operator is given by the Identity operator. This assumption corresponds to assuming a constant velocity model and zero-offset time to depth converted data. The assumption also transforms Eq. 1 to a deconvolution problem. The forward problem becomes:

$$\mathbf{y} = \mathbf{Am} + \mathbf{n}, \tag{2}$$

Given $\mathbf{A}$ and $\mathbf{y}$, we need to find $\mathbf{m}$. Since the early 80's, researchers have cast this problem as a $\ell_1$-norm minimization (Taylor et al., 1979; Oldenburg et al., 1981), where the reflectivity is assumed to be made up of spikes. In recent work by Felix Herrmann, it was shown that the assumption of spiky reflectivity is too limited to describe seismic reflectivity (Herrmann, 2005). This means that in cases where the reflectivity is not spiky, spiky deconvolution may fail (Herrmann, 2005). In our approach, we show that the non-spiky reflectivity is still sparse in the curvelet-domain and that this sparsity can be exploited while solving the deconvolution problem. We start with a brief introduction to curvelets, followed by a presentation of our algorithm and application to synthetic data.

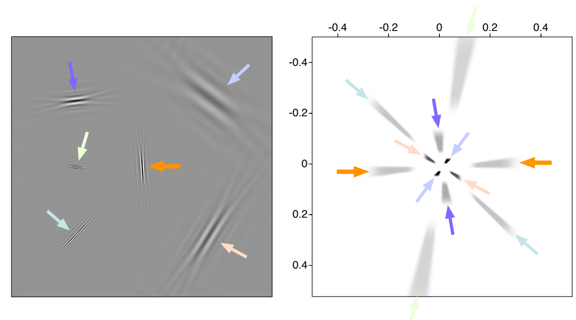


Figure 1: A few curvelets in both spatial (left) and frequency domain (right) (Adapted from Herrmann and Hennenfent, 2008).

## CURVELETS

Curvelets are amongst one of the latest members of the family of multiscale and multidirectional transforms (Candés et al., 2006). They are tight frames (redundant basis) with moderate redundancy. A curvelet is strictly localized in frequency and pseudo-localized in space (have a rapid spatial decay). In the physical domain, curvelets look like little plane waves that are oscillatory in one direction and smooth in other perpendicular directions. Different curvelets at different frequencies and angles are shown in Fig. 1. The construction of curvelets is such that any object with wavefront like structure (e.g seismic images) can be represented by a few significant curvelet coefficients (Candés et al., 2006).

## METHOD

The deconvolution problem with transform-domain sparsity can be cast into the following constrained optimization problem:

$$\tilde{\mathbf{x}} = \arg\min_{\mathbf{x}} ||\mathbf{x}||_1 \quad \text{s.t.} \quad ||\mathbf{y} - \mathbf{AS}^H\mathbf{x}||_2 \leq \varepsilon, \tag{3}$$

where $\tilde{\mathbf{x}}$ represents the estimated transform coefficient vector, $\mathbf{S}^H$ is the transform synthesis operator and $\varepsilon$ is proportional to the noise level. By solving Eq. 3, we try to find the sparsest set of transform coefficients which explains the data within

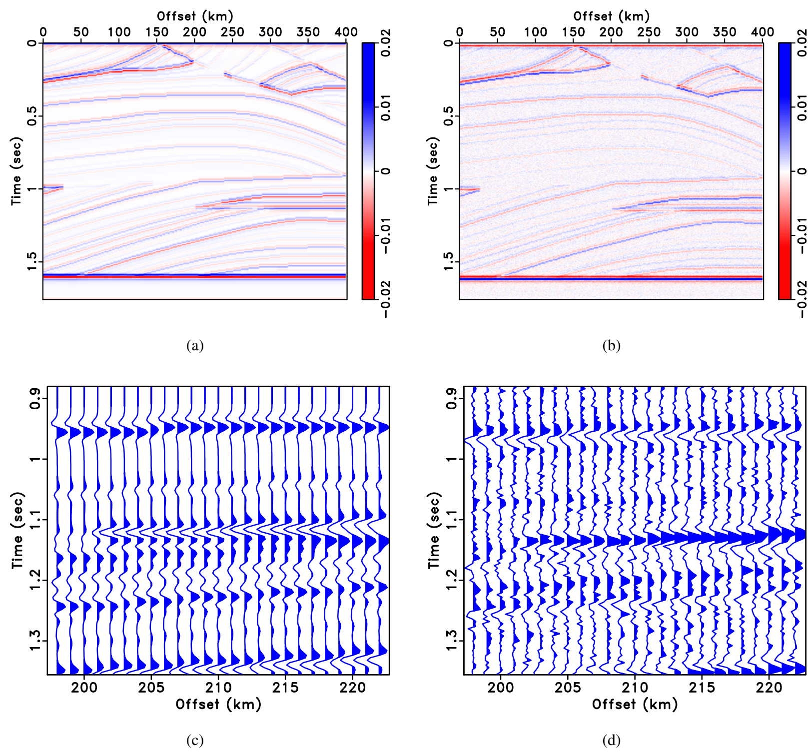


Figure 2: Data and reflectivity model. (a) Original reflectivity. (b) Noisy data ($\sigma$=0.01). Zoom-in plot of (c) original reflectivity and (d) data.

the noise level (Hennenfent et al., 2005). The final estimated reflectivity is given by $\tilde{\mathbf{m}} = \mathbf{S}^H\tilde{\mathbf{x}}$. In our case, the above constrained optimization problem (Eq. 3) is solved by a series of the following unconstrained optimization problem (Herrmann and Hennenfent, 2008):

$$\tilde{\mathbf{x}} = \arg\min_{\mathbf{x}} ||\mathbf{y} - \mathbf{A}\mathbf{S}^H\mathbf{x}||_2 + \lambda||\mathbf{x}||_1, \tag{4}$$

where $\lambda$ is the regularization parameter that determines the trade-off between data consistency and the sparsity. We solve a series of such problems (Eq. 4) starting with high $\lambda$ and decreasing the value of $\lambda$ until $||\mathbf{y} - \mathbf{A}\mathbf{S}^H\mathbf{x}||_2 \approx \varepsilon$, which corresponds to the solution of our optimization problem (Lustig et al., 2007). The lowering of $\lambda$ is done in a controlled way so that we reach the optimum $\lambda$ very rapidly using the SPG$\ell_1$ algorithm (van den Berg and Friedlander, 2008; Hennenfent et al., 2008). Details on the algorithm can be found in the SPG$\ell_1$ Technical report (van den Berg and Friedlander, 2008). In the case of additive white Gaussian noise with standard deviation $\sigma$, the square norm of error $||\mathbf{n}||_2^2$ is a chi-square random variable with mean $\sigma^2 N$ and standard deviation $\sigma^2\sqrt{2N}$, where $N$ is the total number of data points (Candés et al., 2005). For this work, we assume that the probability of $||\mathbf{n}||_2^2$ exceeding its mean plus two standard deviations is small. The maximum $||\mathbf{n}||_2^2$ within two standard deviations is given by $\sigma^2(N + 2\sqrt{2N})$. Thus, we solve Eq. 3 with $\varepsilon^2 = \sigma^2(N + 2\sqrt{2N})$.

## SPARSITY IN THE CURVELET DOMAIN

For this work, we use the reflectivity model which is a small section of smooth Marmousi model. The normalized reflectivity model is shown in Fig. 2. Notice that the reflectivity model is not made up of spikes. Fig. 3 shows the partial reconstruction of the reflectivity with 1 % of the largest amplitude-sorted coefficients of different transforms. We can see that curvelet reconstruction is better compared to Fourier and wavelets. The transform domain should be chosen such that the reflectivity can be represented by relatively few significant coefficients. Considering the above-mentioned facts, we choose $\mathbf{S}^H = \mathbf{C}^H$, where $\mathbf{C}^H$ is the curvelet synthesis operator .

## RESULTS

Noisy data is obtained by convolving a Ricker wavelet (central frequency=25 Hz) with the reflectivity model followed by addition of random Gaussian noise ($\sigma$=0.01). Fig. 2 shows the data, model and zoom-in plot of the target area. We apply our algorithm to the noisy data to estimate the reflectivity. For comparison, we also do spiky deconvolution on the same data for which $\mathbf{S}^H = \mathbf{I}$, where $\mathbf{I}$ is the Identity operator. We keep the same $\varepsilon$ (noise level estimate) for fair comparison. Fig. 4 shows the estimated reflectivity with spiky deconvolution algorithm ($\mathbf{S}^H = \mathbf{I}$) and our curvelet-regularized deconvolution ($\mathbf{S}^H = \mathbf{C}^H$). For more detailed comparison, zoom-in on tar-

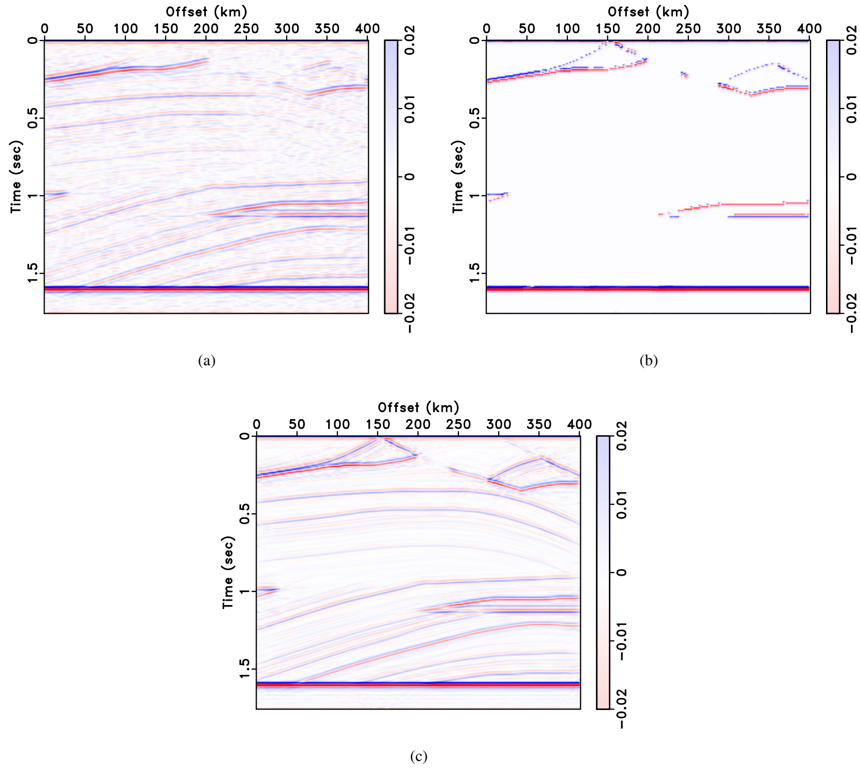


Figure 3: Partial reconstruction in different transform domains. Original reflectivity reconstructed from its 1% amplitude-largest (a) Fourier, (b) wavelet and (c) curvelet coefficients. The curvelet reconstruction is clearly the most accurate approximation.

get area for the original and estimated model is also shown in Fig. 4. Comparing Figs. 4(b), 4(c) and 4(d), we can say that the curvelet estimated model resembles the original model, however the spiky estimate seems unclear due to presence of noise. The curvelet estimated model improves the resolution of the pinch-out at 1.1 seconds which is unclear in the data and spiky estimate of the model. In case of spiky deconvolution, the algorithm tries to estimate a model with series of spikes which explains the data (see Fig. 4(d)). However, in this case the reflectivity is no longer made of spikes and thus spiky deconvolution fails. On the other hand, our curvelet-regularized deconvolution algorithm yields better results by exploiting the continuity along reflectors as shown in Fig. 4(c).

## CONCLUSIONS

In this paper, we showed how non-spiky reflectivity can be recovered by exploiting the continuity along the reflectors by promoting curvelet-domain sparsity. Our algorithm is able to recover the frequency components which gets degraded by noise and convolution operator. The assumption of spiky reflectivity is too limited and may not be valid in all cases and the traditional algorithms may not perform well. Thus, sparsity of such type of reflectivity in the curvelet-domain is a strong prior which we can use as part of our deconvolution algorithm. The next step of our research will be to extend this algorithm to do simultaneous migration and deconvolution for non-spiky reflectivity model exploiting the transform domain sparsity.

## ACKNOWLEDGMENTS

This work was in part financially supported by the NSERC Discovery Grant 22R81254 and CRD Grant DNOISE 334810-05 of F.J. Herrmann and was carried out as part of the SINBAD project with support, secured through ITF, from the following organizations: BG Group, BP, Chevron, ExxonMobil and Shell.

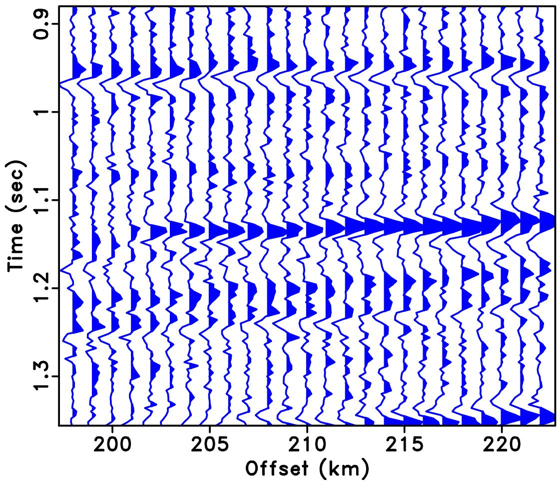


(a)

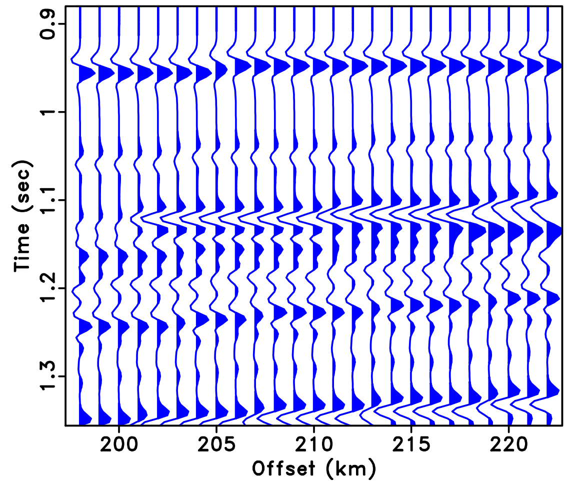


(b)

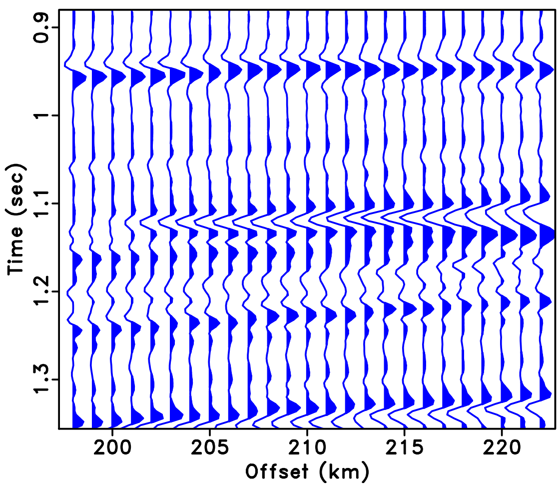


(c)

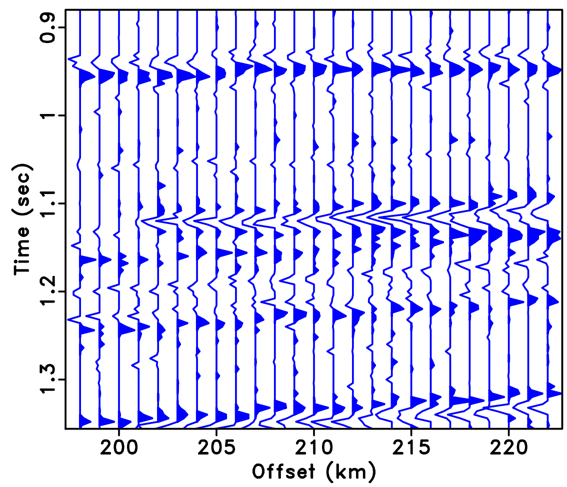


(d)

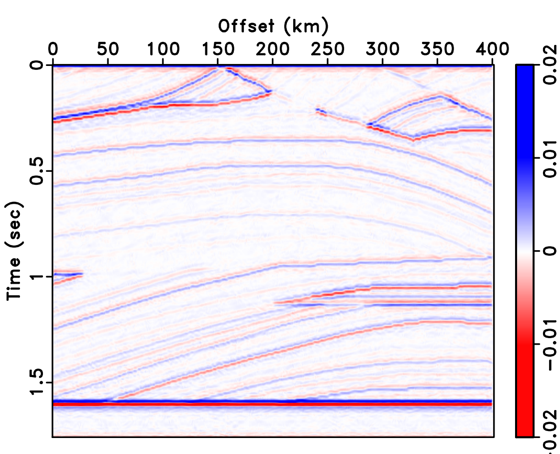


(e)

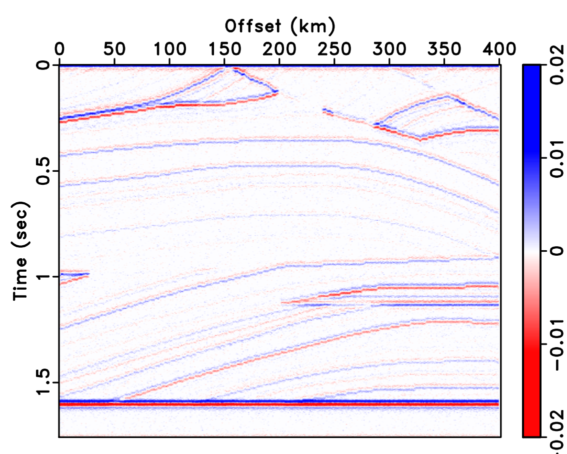


(f)

Figure 4: Zoom-in plot of (a) data, (b) original reflectivity, (c) curvelet estimated reflectivity and (d) spiky estimated reflectivity. Full image of estimated reflectivity (e) with curvelets and (f) spiky deconvolution algorithm.

## REFERENCES


Candés, E., L. Demanet, D. Donoho, and L. Ying, 2006, Fast discrete curvelet transforms: Multiscale Modeling and Simulation, **5**, 861–899.

Candés, E., J. Romberg, and T. Tao, 2005, Stable signal recovery from incomplete and inaccurate measurements: Comm. Pure Appl. Math., **59**, 1207–1223.

De Roeck, Y., 2002, Sparse linear algebra and geophysical migration: A review of direct and iterative methods: Numerical Algorithms, **29**, 283322.

Hennenfent, G., F. J. Herrmann, and R. Neelamani, 2005, Sparseness-constrained seismic deconvolution with Curvelets: Presented at the CSEG National Convention.

Hennenfent, G., E. van den Berg, M. P. Friedlander, and F. J. Herrmann, 2008, New insights into one-norm solvers from the pareto curve: Geophysics.

Herrmann, F. J., 2005, Seismic deconvolution by atomic decomposition: a parametric approach with sparseness constraints: Integr. Computer-Aided Eng., **12**, 69–91.

Herrmann, F. J. and G. Hennenfent, 2008, Non-parametric seismic data recovery with curvelet frames: Geophysical Journal International, **173**, 233–248.

Lustig, M., D. L. Donoho, and J. M. Pauly, 2007, Sparse MRI: The application of compressed sensing for rapid MR imaging: Magnetic Resonance in Medicine. (In press. `http://www.stanford.edu/~mlustig/SparseMRI.pdf`).

Oldenburg, D. W., S. Levy, and K. P. Whittall, 1981, Wavelet estimation and deconvolution: Geophysics, **46**, 1528–1542.

Taylor, H. L., S. C. Banks, and J. F. McCoy, 1979, Deconvolution with $l_1$-norm: Geophysics, **44**, 39–52.

van den Berg, E. and M. P. Friedlander, 2008, Probing the Pareto frontier for basis pursuit solutions: Technical Report TR-2008-01, UBC Computer Science Department. (`http://www.optimization-online.org/DB_HTML/2008/01/1889.html`).